Unsteady state flux response: a method to determine the nature of the solute and gel layer in membrane filtration

Karode, S. L.

Publisher's version / Version de l'éditeur:

Journal of Membrane Science, 188, 2001

ELSEVIER

Journal of Membrane Science 188 (2001) 9–20

journal of MEMBRANE SCIENCE

www.elsevier.nl/locate/memsci

Unsteady state flux response: a method to determine the nature of the solute and gel layer in membrane filtration

Sandeep K. Karode*

National Research Council of Canada, ICPET, M-12, Room 145, Montreal Road Campus, Ottawa, Ont., Canada K1A 0R6

Received 5 September 2000; received in revised form 27 October 2000; accepted 27 October 2000

Abstract

The unsteady-state permeate flux response to a step change in transmembrane pressure is shown to result in unique flux–pressure profiles for the three types of solutes common in membrane ultrafiltration (UF): (a) solutes which exert an osmotic pressure but do not form a 'gel'; (b) solutes which do not exert an osmotic pressure but form a 'gel' and (c) solutes which exert an osmotic pressure and also form a 'gel'. It is also shown that for stirred cell UF, changes in the bulk feed solution properties (concentration, volume) are negligible on the time scale needed to attain a stable permeate flux. Unsteady-state permeate flux measurements could therefore be made at short filtration times so that the results would not be masked by changes in bulk properties.

Keywords: Ultrafiltration; Model; Concentration polarization; Gel; Osmotic pressure; Unsteady-state

1. Introduction

Membrane ultrafiltration (UF) and microfiltration are both known to exhibit the phenomenon of limiting flux. The permeate flux is found to increase with increasing transmembrane pressure till a critical value of transmembrane pressure. At higher values of transmembrane pressure, the permeate flux does not increase further. This is usually explained by the formation of a 'gel' layer of rejected particles, which forms on the feed surface of the membrane.

The solutes being ultrafiltered can be broadly classified into two categories: those which exert an osmotic pressure (like dextran, bovine serum albumin (BSA)) and those which do not (like bentonite, silica). Depending on the variation of osmotic pressure with solute concentration and the hydrodynamic operating conditions, the solutes may or may not form a 'gel' layer when ultrafiltered using completely retentive membranes.

van Oers et al. [1] reported experimental stirred cell UF data for dextran and silica using totally retentive membranes. They measured permeate flux as a function of time for sudden variation of transmembrane pressure. However, as the analysis in this work will show, their measurements were for long times, where the unsteady-state response of the permeate flux to sudden variation in transmembrane pressure were masked by a corresponding increase in the feed bulk concentration. From the time scale of such quasi-steady responses, it was concluded that the build-up of a gel layer of silica particles takes about 1 h while for dextran the concentration polarization layer builds-up within 1 min.

In this study, the unsteady-state model of van Oers et al. [1] is rigorously solved incorporating the variation of the feed bulk volume and concentration as a

* Tel.: +1-613-990-4967; fax: +1-613-941-2529.
E-mail address: sandeep.karode@nrc.ca (S.K. Karode).

0376-7388/01/$ – see front matter
PII: S0376-7388(00)00644-X

Nomenclature

A_m	membrane area (m^2)
C	concentration ($kg\,m^{-3}$)
C_g	'gel' concentration ($kg\,m^{-3}$)
d_p	diameter of solute (m)
D_b	solute diffusivity in polarization boundary layer ($m^2\,s^{-1}$)
J_s	solvent (water) flux ($m^3\,m^{-2}\,s$)
k	mass transfer coefficient (D_b/δ_{pol}) ($m\,s^{-1}$)
ΔP	transmembrane pressure (kPa)
R_g	hydraulic resistance of 'gel' (m^{-1})
R_H	hydraulic resistance of system (m^{-1})
R_m	hydraulic resistance of membrane (m^{-1})
t	time (s)
V_f	feed volume (m^3)
x	spatial coordinate within polarization boundary layer (m)

Greek letters

δ_g	thickness of 'gel' layer (m)
δ_{pol}	thickness of polarization layer (m)
ε_g	porosity of 'gel' layer (0.37)
π	osmotic pressure of solute (Pa)
ρ	solute density ($kg\,m^{-3}$)

Subscripts and superscripts

*	non-dimensional
f	bulk feed
0	initial

function of time. The model is then used to predict true unsteady-state responses to sudden transmembrane pressure changes for three candidate cases: (i) dextran UF where the solute exerts an osmotic pressure but does not form a 'gel' at normal UF transmembrane pressures; (ii) silica UF where the solute does not exert an osmotic pressure but forms a 'gel' and (iii) BSA UF where the solute exerts an osmotic pressure and also forms a 'gel'. It will be shown that from the nature of the flux response as a function of transmembrane pressure, each of the above three cases can be uniquely identified.

2. Model

Consider a stirred UF cell with a membrane area A_m and initial concentration and volume of C_{f0} and V_{f0}, respectively. For a totally retentive membrane, the time variation of the volume (V_f) and concentration (C_f) in the bulk of the UF cell can be written as

$$\frac{dV_f}{dt} = -J_s A_m \tag{1}$$

$$\frac{dC_f}{dt} = J_s A_m \frac{C_f}{V_f} \tag{2}$$

where J_s is the solvent (water) flux. The concentration polarization layer adjacent to the membrane surface can be schematically represented as shown in Fig. 1. Within the concentration polarization layer, the governing equation for the concentration of the solute can be written as [1]

$$\frac{\partial C}{\partial t} = -J_s \frac{\partial C}{\partial x} + D_b \frac{\partial^2 C}{\partial x^2} \tag{3}$$

where, C is the concentration in the polarization (CP) layer, D_b the solute diffusivity in the CP layer, x the coordinate perpendicular to the membrane as shown in Fig. 1.

Eq. (3) is solved with the following initial and boundary conditions.

$$t = 0, \qquad 0 \le x \le \delta_{pol}, \qquad C = C_{f0} \tag{4a}$$

$$t > 0, \qquad x = 0, \qquad C = C_f \tag{4b}$$

$$t > 0, \qquad x = \delta_{pol}, \qquad J_s C\Big|_{x=\delta_{pol}} = D_b \frac{\partial C}{\partial x}\Big|_{x=\delta_{pol}} \tag{4c}$$

The permeate flux can be calculated using the osmotic pressure model [1].

$$J_s = \frac{\Delta P - \Delta\pi}{\mu(R_H)} \tag{5}$$

where ΔP is the transmembrane (feed to permeate) pressure drop, $\Delta\pi$ the osmotic pressure difference between the feed surface and the permeate surface of the membrane, μ the solvent viscosity, R_H is the hydraulic resistance of the system. Before the formation of the 'gel' layer, only the membrane offers any hydraulic resistance (R_m) to the permeate flow. After

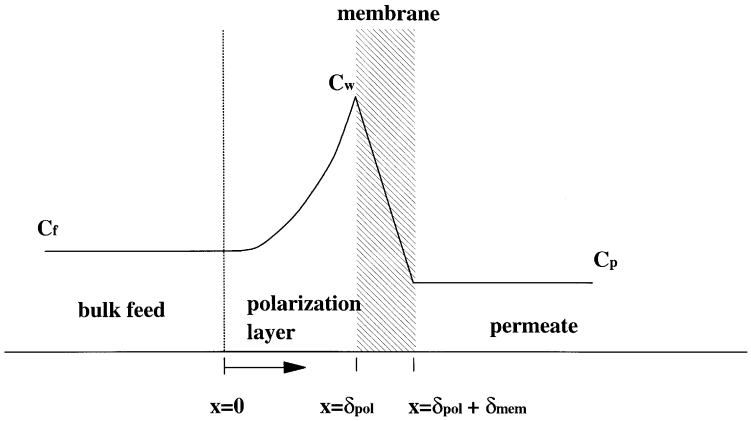

Fig. 1. Schematic of a concentration polarization boundary layer.

the formation of the 'gel' layer, there is an additional resistance due to this layer of accumulated particles. This hydraulic resistance of the 'gel' layer of particles can be calculated using the Kozeny–Carmen equation.

$$R_g = 180\frac{(1-\varepsilon_g)^2}{d_p^2\varepsilon_g^3}\delta_g \tag{6}$$

where d_p is the diameter of the particle and δ_g is the thickness of the gel layer with a porosity of ε_g.

The rate of growth of the 'gel' layer thickness can be calculated by a mass balance as follows.

$$\frac{\partial\delta_g}{\partial t} = J_s - \left(\frac{D_b}{C_g}\right)\left.\frac{\partial C}{\partial x}\right|_{x=\delta_{pol}} \tag{7}$$

The following non-dimensional variables can be defined

$$C^* = \frac{C}{C_{f0}}, \qquad C_f^* = \frac{C_f}{C_{f0}}, \qquad V_f^* = \frac{V_f}{V_{f0}},$$
$$t^* = \frac{t}{\tau}, \qquad \tau = \frac{\delta_{pol}^2}{D_b}, \qquad x^* = \frac{x}{\delta_{pol}},$$
$$\delta_g^* = \frac{\delta_g}{\delta_{pol}} \tag{8}$$

Non-dimensionalizing Eqs. (1)-(7) using the above-defined variables we have

$$\frac{dV_f^*}{dt^*} = -\frac{J_s A_m}{V_{f0}}\tau \tag{9}$$

$$\frac{dC_f^*}{dt^*} = \frac{J_s A_m}{V_{f0}}\frac{C_f^*}{V_f^*} \tag{10}$$

$$\frac{\partial C^*}{\partial t^*} = -\frac{J_s\delta_{pol}}{D_b}\frac{\partial C^*}{\partial x^*} + \frac{\partial^2 C^*}{\partial x^{*2}} \tag{11}$$

$$\frac{d\delta_g^*}{dt^*} = \frac{J_s\delta_{pol}}{D_b} - \frac{1}{C_g^*}\left.\frac{\partial C^*}{\partial x^*}\right|_{x=\delta_{pol}} \tag{12}$$

The initial conditions for Eqs. (9)–(12) are given by

$$V_f^* = 1, \qquad C_f^* = 1, \qquad 0 \le x^* \le 1,$$
$$C^* = 1, \qquad \delta_g^* = 0 \tag{13}$$

The boundary conditions for Eq. (11) are given by

$$x^* = 0, \qquad C^* = C_f^* \tag{14a}$$

$$x^* = 1, \qquad C^*\big|_{x^*=1} = \frac{D_b}{J_s\delta_{pol}}\left.\frac{\partial C^*}{\partial x^*}\right|_{x^*=1} \tag{14b}$$

Using the virial coefficient expression [1] for the osmotic pressure, the solvent flux can be written as

$$J_s = \frac{\Delta P - A_1 C\,|_{x^*=1} - A_2 C|^2_{x^*=1} - A_3\,C|^3_{x^*=1}}{\mu(R_m + R_g)} \tag{15}$$

where A_{1-3} are constants relating the osmotic pressure of the solute to a polynomial expansion in its concentration (C).

Eqs. (9)–(15) completely define the system. Once the system parameters like ΔP and the stirring speed (or mass transfer coefficient) are fixed, solving Eqs. (9)–(15) simultaneously, we can predict the membrane surface concentration and the permeate flux.

3. Method of solution

In order to simultaneously solve the above governing equations, the non-dimensional boundary layer thickness was discretized into 100 equally spaced intervals such that $x^* = 0$ corresponded to the first grid point and $x^* = 1$ corresponded to grid point number 101. Discretizing Eq. (11) using the central finite difference then results in 99 first order ordinary differential equations (I-ODEs) for the concentration profile within the polarization layer.

Discretizing Eq. (14b) using the backward difference method then results in a non-linear algebraic equation to be solved for the membrane feed surface concentration ($C^*|_{x^*=1}(C_m^*)$). This was solved by the Newton–Raphson method. From the wall concentration, the porosity of the accumulated particle layer can be calculated using the density of the particles as follows.

$$\varepsilon_g = 1 - \frac{C_{f0}C^*|_{x^*=1}}{\rho} \tag{16}$$

where ρ is the solute density. Hence, the 101 I-ODEs before 'gel' formation and the 102 I-ODEs including Eq. (12) after 'gel' formation were integrated using the 4th order Runge–Kutta integration scheme. After each time integration, the non-linear algebraic equation resulting from the discretization of Eq. (14b) was solved so as to calculate the surface concentration. This cycle of integration was carried out till steady state.

4. Hydrodynamic and solute parameters

The model parameters are summarized in Table 1. The membrane hydraulic resistance, the viscosity and the parameters for dextran and silica were taken from van Oers et al. [1]. The virial coefficients for calculating the osmotic pressure for BSA were taken from Vilker et al. [2]. The size and density of BSA were taken from Opong and Zydney [3].

The extent of the polarization layer was calculated by assuming a typical mass transfer coefficient ($k = D_b/\delta_{pol}$) of 1 $\mu m\,s^{-1}$ as reported by van Oers et al. [1]. Typical values of membrane area (A_m) and the initial volume (V_{f0}) for stirred cell UF were also taken from van Oers et al. [1]. The 'gel' layer porosity was set to that of the maximum packing for solid spheres equal to 0.37.

5. Model predictions and discussion

The model developed in this work has been previously verified against literature experimental data [4]. In this study, we will now apply this model to unsteady-state flux response to three generic kinds of solutes namely: (i) a solute that exerts an osmotic pressure but does not form a 'gel' at normal UF transmembrane pressures (Dextran T70); (ii) a solute that does not exert an osmotic pressure but forms a 'gel' (silica) and (iii) a solute that exerts an osmotic pressure and also forms a 'gel' at normal UF transmembrane pressures (BSA).

Table 1
Hydrodynamic and solute parameters

A_m	$144 \times 10^{-4}\,m^2$
C_{f0}	7–28 $kg\,m^{-3}$
k	$10^{-6}\,m\,s^{-1}$
R_m	$1.88 \times 10^{13}\,m^{-1}$
V_{f0}	$2 \times 10^{-3}\,m^3$
ε_g	0.37
μ	10^{-3} Pa s

Solute parameters	D_b ($m^2\,s^{-1}$)	ρ ($kg\,m^{-3}$)	d_p (nm)	A_1 (Pa $m^3\,kg^{-1}$)	A_2 (Pa $m^6\,kg^{-2}$)	A_3 (Pa $m^9\,kg^{-3}$)
Dextran T70	4.6×10^{-11}	1125	5	37.5	0.752	76.4×10^{-4}
BSA	6.75×10^{-11}	1100	4.5	36.5	0.336	1.09×10^{-3}
Silica	3.59×10^{-11}	2250	12	0.0	0.0	0.0

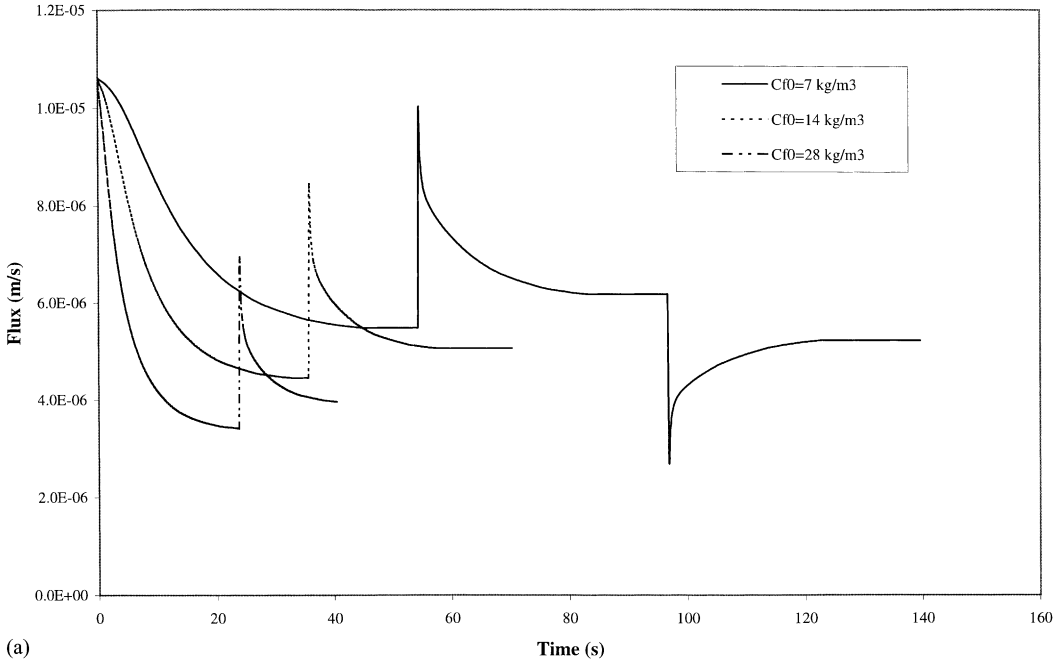

(a)

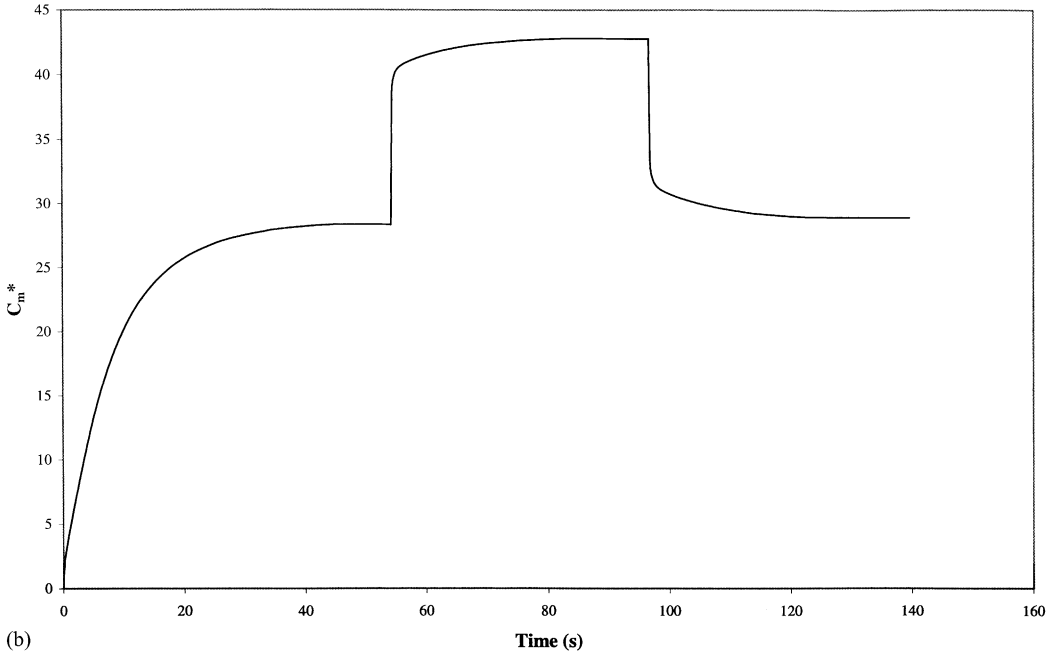

(b)

Fig. 2. (a) Unsteady-state permeate flux as a function of time for Dextran T70 using parameters listed in Table 1 for three different initial bulk feed concentrations (ΔP values given in the text). (b) Non-dimensional membrane feed surface concentration as a function of time for Dextran T70 UF ($C_{f0} = 7\,kg\,m^{-3}$; $\Delta P = 200/400/200\,kPa$). (c) Steady state non-dimensional concentration profile within the concentration polarization boundary layer for Dextran T70 UF for various values of ΔP ($C_{f0} = 7\,kg\,m^{-3}$).

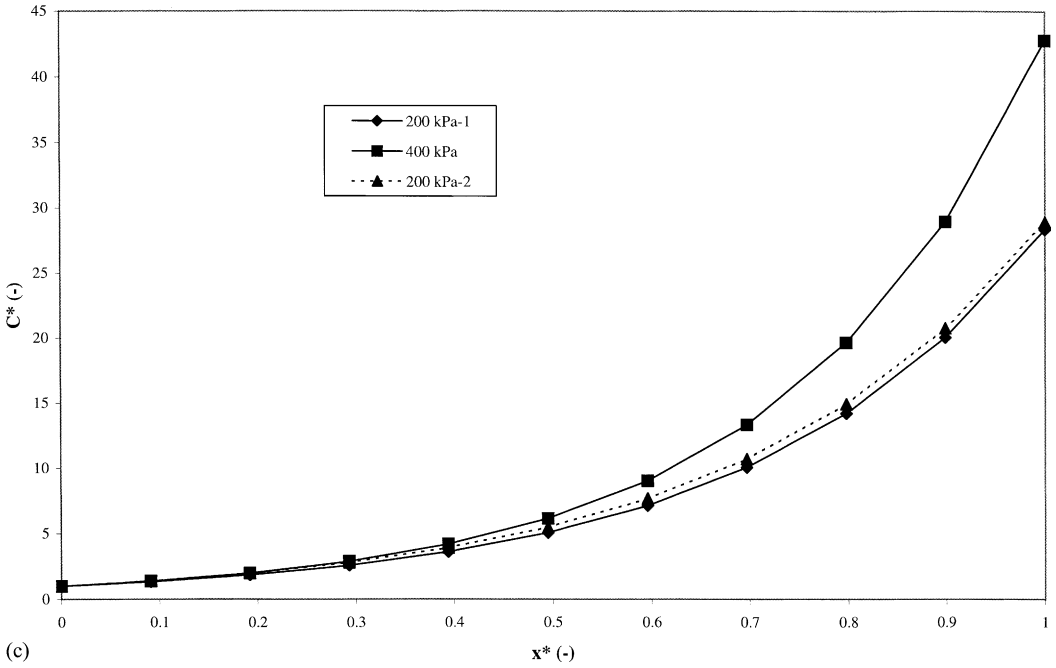

Fig. 2 (*Continued*).

Using the parameters listed in Table 1, an analysis of Eqs. (9) and (10) show that on the time scale required to attain a stable permeate flux, the rate of change of the bulk feed concentration and volume of solute is negligible. Hence, if permeate flux measurements are made so as to measure the actual unsteady-state values, effects of the variation of the bulk concentration and volume in stirred cell UF can be neglected. The bulk volume and concentration change was actually found to be negligible for the entire range of parameters studied in this work.

In all the simulations using the parameters listed in Table 1, the mass transfer coefficient was kept the same for each of the three solutes so as to enable comparison under identical mass transfer conditions.

Fig. 2a shows the unsteady-state permeate flux as a function of time for Dextran T70 UF with the parameters listed in Table 1 for three different initial bulk feed concentrations. The starting transmembrane pressure ($t = 0$) was set to 200 kPa for all three cases. After steady state was reached, ΔP was increased to 400 kPa to predict the unsteady-state flux response. For the case of 7 kg m^{-3}, after steady state was reached for 400 kPa, the pressure was then again lowered to 200 kPa. Hence, the pressure cycle for the case of 7 kg m^{-3} was 200/400/200 while that for the other two cases was 200/400. As can be seen from Fig. 2a, the time required to reach steady state decreases as the feed concentration increases.

For each of the three concentrations, an increase in ΔP results in a corresponding increase in steady state permeate flux. Further for the cycle 200/400/200, a decrease in pressure back to 200 kPa results in a reversible decrease in the permeate flux corresponding to the steady state value obtained by starting at 200 kPa. Fig. 2b and c, respectively, show the model prediction of the non-dimensional membrane surface concentration (C^*_m) and the steady state non-dimensional concentration profile ($C^*(x^*)$) within the boundary layer for the pressure cycle of 200/400/200 ($C_{f0} = 7$ kg m^{-3}). As can be seen from Fig. 2b, the non-dimensional surface concentration is well below the non-dimensional 'gel' concentration ($C^*_g = 101.25$) and hence is a function of the transmembrane pressure and the system hydrodynamics. It is therefore reversible for the pressure cycle of 200/400/200 and so is the steady state concentration profile within the boundary layer as shown in Fig. 2c.

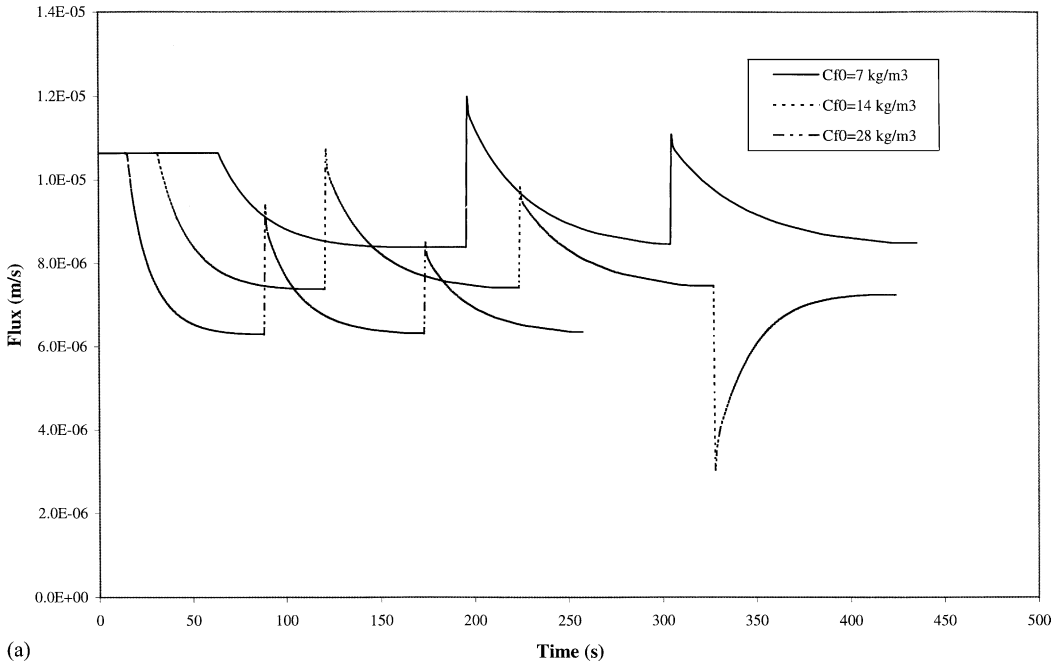

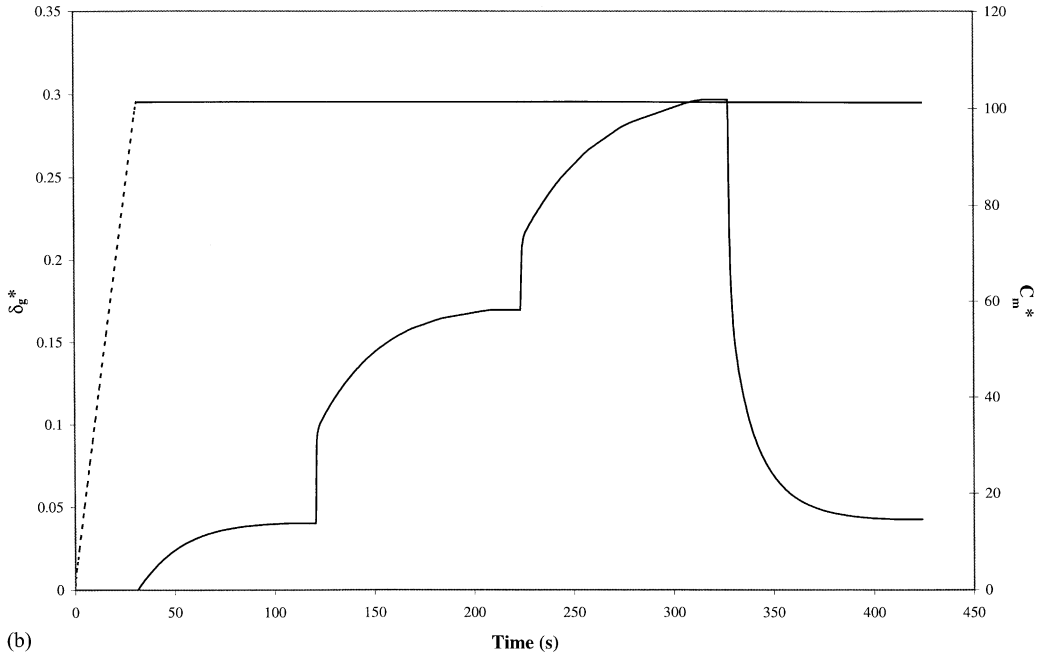

Fig. 3. (a) Unsteady-state permeate flux as a function of time for silica UF using parameters listed in Table 1 for three different initial bulk feed concentrations (ΔP values given in the text). (b) Non-dimensional membrane feed surface concentration (dotted line) and 'gel' layer thickness (solid line) as a function of time for silica UF ($C_{f0} = 14\,\mathrm{kg\,m^{-3}}$; $\Delta P = 200/400/600/200\,\mathrm{kPa}$).

The sudden drop in the permeate flux for a pressure change of 400/200 (in Fig. 2a) can be explained as being due to a sudden drop in the effective driving pressure. The steady state effective driving pressure ($\Delta P - \Delta\pi$) at 400 kPa was 116 kPa which drastically reduces to 51.6 kPa at 200 kPa resulting in a sharp drop in permeate flux.

Hence, a solute capable of exerting an osmotic pressure but not forming a 'gel' layer exhibits a gradual flux decline with time followed by a reversible steady state permeate flux for a sudden increase followed by a decrease to the initial value of transmembrane pressure ΔP.

Fig. 3a shows the unsteady-state flux for silica UF using the parameters listed in Table 1 for three different initial bulk feed concentrations. The starting pressure in all cases was 200 kPa. The figure shows the unsteady-state flux response for a pressure cycle of 200/400/600 for $C_{f0} = 7$ and $28\,kg\,m^{-3}$ and a cycle of 200/400/600/200 for $C_{f0} = 14\,kg\,m^{-3}$.

As can be seen from Fig. 3a, there is a finite period of constant flux for silica UF at short filtration times. This time period of constant flux decreases as the initial bulk feed concentration increases. As soon as the concentration of rejected particles on the membrane surface exceeds the 'gel' concentration, there is an additional resistance to permeate flux and hence the flux starts decreasing as a function of time. What is interesting is that the steady state value of the permeate flux is independent of the transmembrane pressure ΔP once a 'gel' layer is formed. A pressure cycle of 200/400 results in a sudden increase in permeate flux which gradually reduces back to the value corresponding to the steady state value at 200 kPa. Such behavior has been experimentally reported recently for filtration of Bentonite particles by Hamachi and Mietton-Peuchot [5].

Fig. 3b shows the non-dimensional membrane surface concentration (C_m^*) and the non-dimensional 'gel' layer thickness (δ_g^*) for a pressure cycle of 200/400/600/200 ($C_{f0} = 14\,kg\,m^{-3}$). As can be seen, once the surface concentration reaches the 'gel' concentration, it does not change with variation of ΔP. Only the 'gel' layer thickness changes with varying

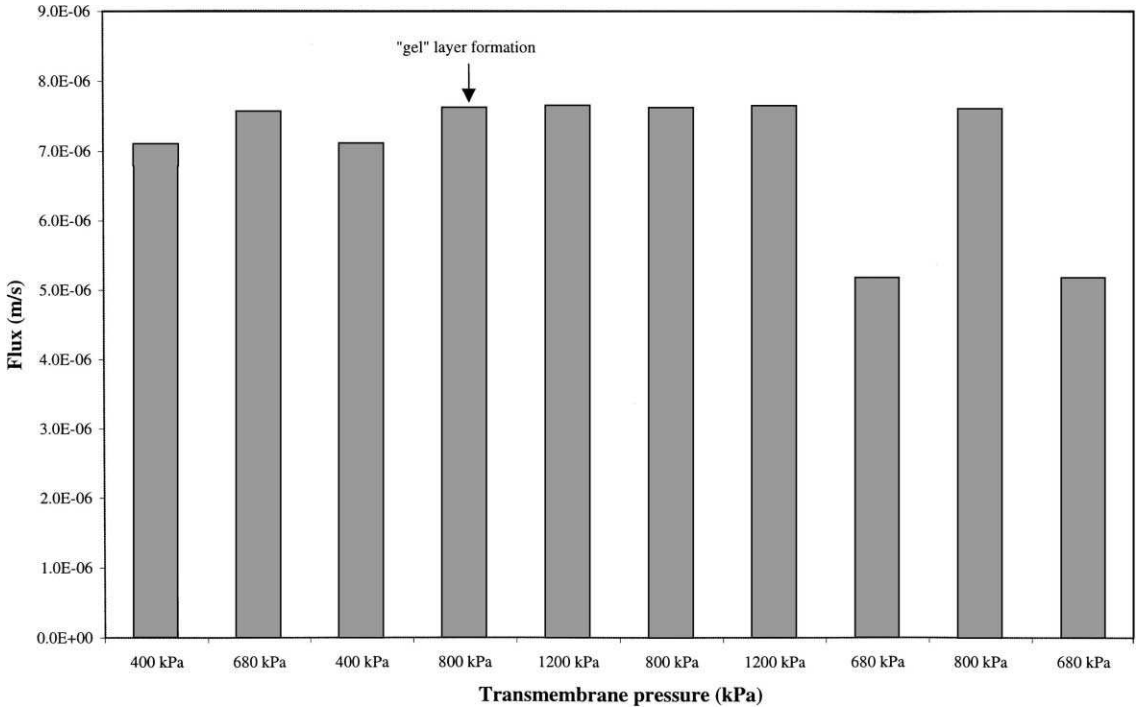

Fig. 4. Steady state permeate flux as a function of ΔP for BSA UF using parameters listed in Table 1 ($C_{f0} = 7\ kg\,m^{-3}$).

transmembrane pressure which results in a corresponding variation in the permeate flux. However, since the growth of the 'gel' layer thickness is dependent on the convective transport of particles (i.e. the permeate flux), the system becomes auto-regulatory, resulting in an invariant steady state permeate flux for silica particles.

Hence, for a solute which does not exert an osmotic pressure, there is a characteristic time ($t_c = D_b(C_g - C_{f0})/J_s^2 C_{f0}$) for which the permeate flux is time-invariant [6]. After this characteristic time, a 'gel' layer forms on the surface of the membrane and the permeate flux decreases with time till a steady state is reached. The system then becomes auto-regulatory and the steady state permeate flux is invariant with either an increase or decrease in transmembrane pressure.

We now consider the third kind of solute (BSA) which exerts an osmotic pressure and which is capable of forming a 'gel' layer for typical transmembrane pressure ranges in UF. Fig. 4 shows the steady state permeate flux as a function of transmembrane pressure for BSA UF using the parameters listed in Table 1 for a initial bulk feed concentration of 7 kg m^{-3}. The unsteady-state flux profile was similar to that for Dextran T70 in that there was no region of constant time invariant flux at short filtration times. As can be seen, for a pressure cycle of 400/680/400, the steady state permeate flux increases and then decreases reversibly to the initial steady state at 400 kPa. Subsequently, when ΔP was increased to 800 kPa, there was a formation of a 'gel' layer and hence for a further increase in ΔP to 1200 kPa, there was no corresponding increase in the steady state permeate flux. A subsequent decrease in ΔP to 800 kPa resulted in the same steady state flux as for the previous cycle of 800 kPa. This is because the thickness of the 'gel' layer adjusted itself to the corresponding drop in ΔP.

However, when ΔP was lowered to 680 kPa (where there was no 'gel' layer formation initially), the steady state permeate flux was much lower than that at the first cycle of 680 kPa. This is different from the case for silica UF where the silica particles did not exert an osmotic pressure. The reason for this corresponding drop in steady state permeate flux is as

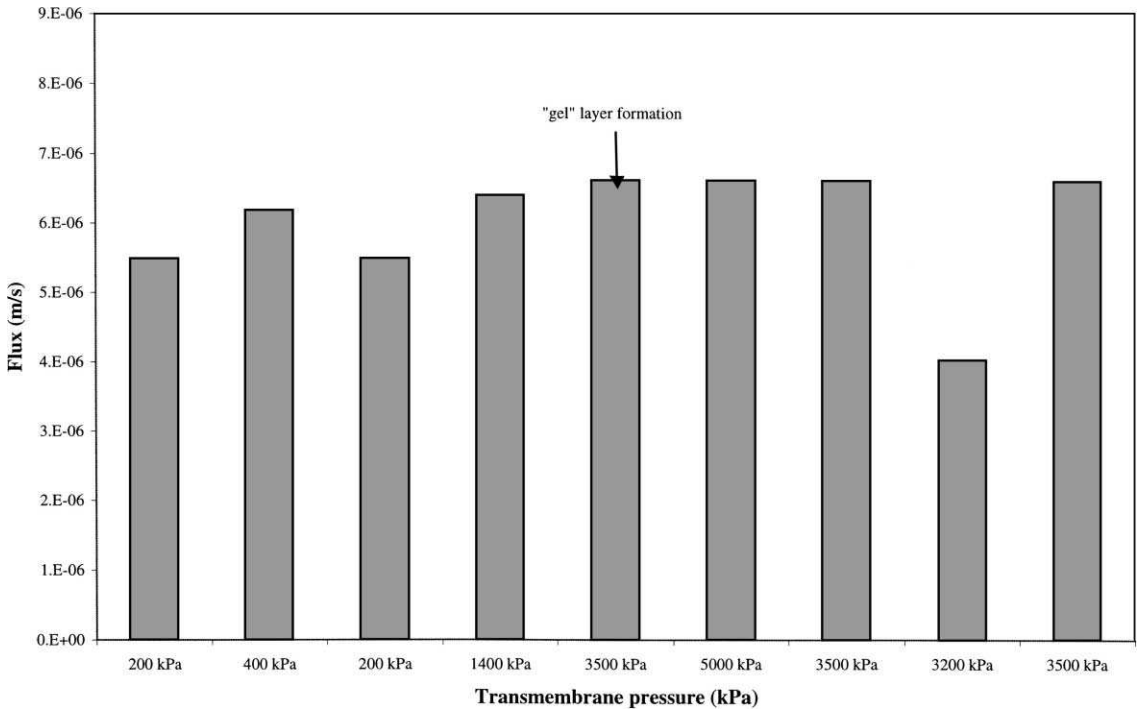

Fig. 5. Steady state permeate flux as a function of ΔP for Dextran T70 UF using parameters listed in Table 1 ($C_{f0} = 7$ kg m^{-3}).

follows. When ΔP is lowered to 680 from 800 kPa, the steady state 'gel' layer thickness reduces to zero (to adjust itself to the lower transmembrane pressure). However, the membrane surface concentration remains constant at the value corresponding to the 'gel' layer. Since the 'gel' layer of rejected particles exert an osmotic pressure, the corresponding steady state permeate flux is lower than that at the first cycle of 680 kPa.

For the first cycle of 680 kPa, there was no 'gel' layer formation and hence the osmotic pressure exerted by the rejected particles at the membrane surface was lesser. Consequently, the steady state permeate flux was higher.

For a subsequent increase in ΔP from 680 to 800 kPa, the permeate flux was found to be the same as that for the earlier cycle of 800 kPa. A further cycle 800/680 resulted in the same steady state value for the second cycle of 680 kPa after the formation of the 'gel' layer.

In order to confirm that this prediction for BSA was not an artifact of the computer code, simulations were carried out for Dextran T70 at unrealistically high values of ΔP. This is shown in Fig. 5 for an initial bulk feed concentration of 7 kg m^{-3} and other parameters for Dextran T70 listed in Table 1. As was shown earlier, there is a reversible flux–pressure relationship at low pressure cycle of 200/400/200 kPa. An increase in ΔP from 200 to 1400 kPa results in an increase in steady state permeate flux. A further increase to 3500 kPa results in a slight increase in permeate flux and the formation of a 'gel' layer. Due to it is high osmotic pressure, at normal operating pressures for UF (<1500 kPa) Dextran T70 would not form a 'gel' layer.

An increase in ΔP above 3500–5000 kPa does not lead to an increase in permeate flux since the 'gel' layer makes the system auto-regulatory. A subsequent reduction of ΔP to 3500 kPa too does not alter the permeate flux since the thickness of the 'gel' layer

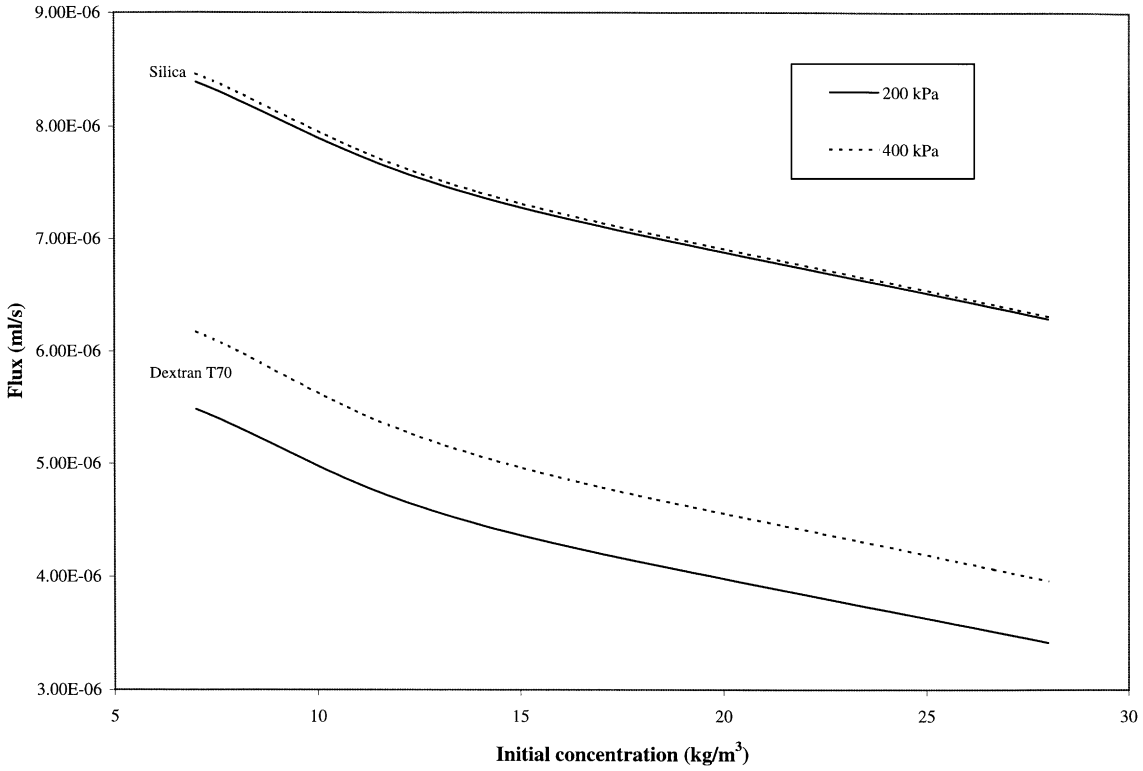

Fig. 6. Steady state permeate flux as a function of initial concentration at two different ΔP values for silica and Dextran T70.

adjusts itself to the change in ΔP. A further decrease in ΔP to 3200 kPa results in an irreversible reduction in the steady state permeate flux with the 'gel' layer thickness dropping to zero but the membrane surface concentration being stationary at the 'gel' value. This is exactly the same trend as was observed for BSA. A subsequent increase in ΔP to 3500 kPa leads to the same steady state flux as for the previous cycle at 3500 kPa.

Therefore, for a solute capable of exerting an osmotic pressure and also forming a 'gel' layer, before the formation of the gel layer there is a reversible flux–pressure relationship; an increase in ΔP leads to an increase in steady state flux while a decease in ΔP to the original value leads to the same steady state flux. After the formation of the 'gel' layer (i.e. after a certain critical value of ΔP), an increase in ΔP does not result in any increase in steady state permeate flux. A subsequent decrease in ΔP below the critical value results in an irreversible reduction in steady state permeate flux.

It is imperative however, to measure the transient unsteady permeate flux as a function of time for each step change in ΔP. If the filtrate flux is measured at long filtration times as was done by van Oers et al. [1], the unsteady-state effects described above would be masked due to change in the bulk feed concentration. Fig. 6 shows the steady state permeate flux for two values of ΔP (200 and 400 kPa) for Dextran T70 and silica as a function of initial bulk feed concentration. As can be seen, for both solutes, an increase in feed concentration leads to a lower steady state flux. Further, since Dextran T70 does not form a 'gel', an increase in ΔP leads to a corresponding increase in permeate flux, whereas the steady state permeate flux is insensitive to ΔP. Hence, if truly unsteady-state measurements are made for step changes in transmembrane pressure ΔP, the nature of the flux-ΔP profile could be analyzed to determine the nature of the 'gel' layer.

6. Conclusions

Unsteady-state permeate flux measurements for step changes in transmembrane pressure are shown to result in unique responses for each of the following three cases: (i) solute which exerts an osmotic pressure but does not form a 'gel' (e.g. Dextran T70); (ii) solute which does not exert an osmotic pressure but forms a 'gel' (e.g. silica particles) and (iii) solute which exerts an osmotic pressure and also forms a 'gel' (e.g. BSA).

For stirred cell UF, the changes in the bulk feed volume and concentration are shown to be negligible for time scales required for the establishment of a steady permeate flux. Measurements made within this time frame would not be masked by changes in the bulk properties (concentration and volume).

The unsteady-state flux response to each of the above three cases is as follows.

1. At the beginning of the filtration, there is a decline in the permeate flux as a function of time till a steady state is reached. After steady state is reached, a step increase in transmembrane pressure results in a sharp increase followed by a gradual decrease to a higher steady state value for the permeate flux. A subsequent reduction in the transmembrane pressure to the original value results in a sharp drop followed by a gradual increase in the permeate flux to stabilize at the same value as for the initial steady state before the step increase in pressure.
2. At the beginning of the filtration, there is a critical time for which the permeate flux is time invariant, during which time, the concentration at the membrane surface increases. After the critical time, a 'gel' layer of accumulated particles causes the permeate flux to decrease with time before attainment of a steady state. A subsequent step increase in transmembrane pressure causes a sharp increase in the permeate flux which gradually decreases to the same steady value before the step increase. A further step decrease in transmembrane pressure results in a sharp drop followed by a gradual rise to the same steady state as before. Hence, in such situations, after the critical time period, the system is self regulatory and the steady permeate flux is independent of the change in transmembrane pressure. This is in line with the recently reported experimental results of Hamachi and Mietton-Peuchot [5].
3. At the beginning of the filtration there is a gradual drop in permeate flux with time before stabilizing at a steady state. A step increase/decrease in transmembrane pressure results in a corresponding reversible increase/decrease in the steady state permeate flux. After a certain critical transmembrane pressure, a step increase in pressure does not result

in any steady state increase in permeate flux. This is indicative of the formation of a 'gel' layer. A subsequent decrease in transmembrane pressure below the critical value results in an irreversible reduction in the steady state permeate flux.

References

[1] C.W. van Oers, M.A.G. Vorstman, W.G.H.M. Muijselaar, P.J.A.M. Kerkhof, Unsteady-state flux behaviour in relation to the presence of a gel layer, J. Membr. Sci. 73 (1992) 231–246.

[2] V.L. Vilker, C.K. Colton, K.A. Smith, The osmotic pressure of concentrated protein solutions: effect of concentration and pH in saline solutions of bovine serum albumin, J. Coll. Int. Sci. 79 (2) (1981) 548–566.

[3] W.S. Opong, A.L. Zydney, Diffusive and convective protein transport through asymmetric membranes, AIChE J. 37 (10) (1991) 1497–1510.

[4] S.K. Karode, T. Courtois, M. Mietton-Peuchot, B.B. Gupta, Protein ultrafiltration: an explanation for negative rejection, J. Membr. Sci. 168 (2000) 75–85.

[5] M. Hamachi, M. Mietton-Peuchot, Experimental investigations of cake characteristics in crossflow microfiltration, Chem. Eng. Sci. 54 (1999) 4023–4030.

[6] S. Redkar, V. Kuberkar, R.H. Davis, Modeling of concentration polarization and depolarization with high frequency backpulsing, J. Membr. Sci. 121 (2) (1996) 229–242.